

1 Distinguishing core and flank facies based on shell fabrics in Lower Jurassic lithiotid shell beds

2 Core and flank facies based on shell fabrics in Lower Jurassic lithiotid shell beds

3

4

5 Valentina Brandolese ^a, Renato Posenato ^a, James H. Nebelsick ^b, Davide Bassi ^{a,*}

6

7 ^a *Dipartimento di Fisica e Scienze della Terra, Università degli Studi di Ferrara, via Saragat 1,*

8 *44122 Ferrara, Italy*

9 ^b *Department of Geosciences, University of Tübingen, Sigwartstr. 10, 72076 Tübingen, Germany*

10

11 *Corresponding author.

12 *E-mail address:* bsd@unife.it (D. Bassi)

13

14

15 *Keywords:*

16 Shallow-water carbonates

17 Shell accumulations

18 Lithiotid bivalves

19 Palaeoecology

20 Taphonomy

21 Pliensbachian

22

23 **ABSTRACT**

24

25 Lower Jurassic larger bivalves, mostly represented by the monospecific lithiotid genera *Lithiotis*,
26 *Cochlearites* and *Lithioperna*, formed large shell accumulations in the shallow-water carbonate
27 Tethyan and Panthalassa margins. A quantitative analysis of lithiotid accumulations from the Trento
28 Platform (northern Italy) was carried out in order to solve the conundrum of distinguishing the
29 distribution of autochthonous and parautochthonous forming lithiotids in the core and flanks of
30 these bivalve accumulation. Various representative accumulations are characterized with respect to
31 taxonomic make up systematic content, shell cover, shell density, orientation and disarticulation of
32 individual shells allowing for autochthonous, parautochthonous or allochthonous individuals to be
33 distinguished within core and flank deposits. *Lithioperna* shows a high shell cover within the
34 accumulation core while that of *Cochlearites* is variable and *Lithiotis* is rare. All three lithiotids
35 occur in high densities in the accumulation flanks. As expected, autochthonous individuals of all

36 three genera are frequent in the accumulation cores where they are preserved in life position. In the
37 flanks, most bivalves are parautochthonous except for *Lithioperna* which can grow in life position.
38 Bivalves in allochthonous shell beds are highly fragmented and disarticulated. The studied traits are
39 potentially useful as proxies for distinguishing core or flank facies when the accumulation does not
40 crop out as a whole.

41

42 **1. Introduction**

43

44 Abundant and well-diversified in different marine habitats, the bivalves are a key-group
45 involved in the biotic recovery after the end-Triassic mass extinction event (e.g., Bambach, 2006;
46 Wignall and Bond, 2008; Mander et al., 2008; Ros and Echevarría, 2012). Their recovery and
47 diversification was very rapid and not geographically homogeneous in comparison with other
48 marine invertebrates (e.g., corals). For instance, they show high origination rates in Argentina
49 already since the uppermost latest early Hettangian (Damborenea et al., 2017), while a nearly
50 instantaneous recovery has been reported in Tibet (Hautmann et al., 2008). Significant
51 diversification is observed among Hettangian marine invertebrates, culminating in the
52 Pliensbachian reappearance of reef organisms/reef biotas/reef habitats/reef ecosystems (Hallam and
53 Wignall, 1997). These organisms/biotas/habitats/ecosystems recorded biotic turnovers, changes in
54 abiotic ocean and regional perturbations (e.g., Dera et al., 2010; Martindale et al., 2019).

55 Sinemurian–lower Toarcian tropical shallow-water communities are distinguished by a
56 unique evolutionary phase of aberrant and frame-building constrictal-growth forms (*sensu* Skelton et
57 al., 1995) represented by the lithiotid bivalves. These include several, not systematically related,
58 gregarious taxa such as *Cochlearites*, *Gervilleioperna*, *Lithiotis*, *Lithioperna*, *Mytiloperna* and
59 *Opisoma*. They thrived along the Tethyan and Phanthalassa margins from northern Africa, through
60 southeast Asia to western America (e.g., Bosellini, 1972; Broglio Loriga and Neri, 1976; Geyer,
61 1977; Lee, 1983; Nauss and Smith, 1988; Buser and Debeljak, 1994; Leinfelder et al., 2002; Fraser
62 et al., 2004; Posenato and Masetti, 2012). Well known lithiotids occur in the Formazione di Rotzo,
63 a shallow-water carbonate succession deposited on the Jurassic Trento Platform of northeastern
64 Italy (e.g., Gümbel, 1871; Tausch, 1890; Böhm, 1891; Reis, 1903; Bosellini and Broglio Loriga,
65 1971; Clari, 1975; Masetti et al., 1998), the objects of this study.

66 Modern accumulations of larger bivalve shells constructed by oysters play an important
67 ecological role on marine substrates, providing habitats for other organisms (e.g., Coen and Grizzle,
68 2016). These accumulations affect in different terms turbidity and nutrient recycling by their filter
69 feeding (Gutiérrez et al., 2003). When the balance between oyster recruitment and mortality rate is

70 higher than the carbonate loss, the accumulations attain vertical relief (e.g., Waldbusser et al., 2011).
71 Reef-building oysters have thus been considered ecosystem engineers (Parras and Casadío, 2006;
72 Gutiérrez et al., 2011). Similar ecological conditions have been reconstructed for the Lower Jurassic
73 lithiotids which formed large shell accumulations in shallow-water carbonate depositional systems
74 (e.g., Bosellini, 1972; Broglio Loriga and Neri, 1976; Chinzei, 1982; Fraser et al., 2004; Posenato
75 and Masetti, 2012; Brame et al., 2019).

76 Studies on these faunas have been focused mostly on systematics (Accorsi Benini and
77 Broglio Loriga, 1977; Accorsi Benini, 1979), functional morphology (i.e., Chinzei, 1982; Seilacher,
78 1984; Accorsi Benini and Broglio Loriga, 1982; Seilacher, 1984; Accorsi Benini, 1985; Broglio
79 Loriga and Posenato, 1996; Savazzi, 1996) and palaeobiogeography (Broglio Loriga and Neri,
80 1976; Fraser et al., 2004) of these faunas. Recent investigations have shown that the lower
81 Pliensbachian faunal distribution took place after the Sinemurian–Pliensbachian eutrophic, poorly
82 oxygenated water phase (Franceschi et al., 2014), and that the extinction of these largest aberrant
83 bivalves occurred at the onset of the early Toarcian oceanic anoxic event (Trecalli et al., 2012;
84 Franceschi et al., 2014; Posenato et al., 2018).

85 Difficulties in distinguishing the lithiotids preserved in indurated limestone have hampered
86 the detailed descriptions of their accumulations and related architecture (i.e., core and flanks), as
87 well as the distinction of autochthonous and parautochthonous individuals. At the outcrop scale,
88 randomly sectioned shells often do not show the diagnostic characters at genus level. Furthermore,
89 the entire accumulation shape rarely crops out completely and the architectural features (i.e., core,
90 flanks as described by Posenato and Masetti, 2012) are poorly known (e.g., Posenato et al., 2018).
91 Although a suite of quantitative methods to describe the rudist accumulations has been so far
92 applied and discussed (e.g., Vilardell and Gili, 2003; Gili et al., 2016), little has been performed for
93 the lithiotid accumulations as far as quantitative methodology is concerned (Posenato et al., 2018).
94 The conundrum of Lower Jurassic lithiotids lies, therefore, in the distinction of (1) the
95 autochthonous and parautochthonous individuals and (2) the accumulation architecture (i.e., core
96 and flanks).

97 Various accumulations containing the monospecific taxa *Lithiotis problematica* Gümbel,
98 1871, *Cochlearites loppianus* (Tausch, 1890) and *Lithioperla scutata* (Dubar, 1948) from the
99 Trento Platform are studied in detail in order to: (1) document different lithiotid accumulations with
100 respect to taxonomic diversity of large bivalves, sedimentary fabric and taphonomy; (2) identify
101 different accumulation types including cores and flanks by quantitative various sedimentary and
102 taphonomic attributes; and (3) distinguish and interpret different taxonomic systematic presence and
103 preservation of autochthonous, parautochthonous or allochthonous bivalves within the architectural
104 features of the accumulations.

105

106 **2. Jurassic lithiotid bivalves**

107

108 The taxonomic identification of lithiotid bivalves at the outcrop scale is difficult because
109 specific shell sections showing diagnostic characters are usually very rare (e.g., Posenato et al.,
110 2018). The most recognizable characters are found in transversal sections of the dorsal body cavity
111 (e.g., Berti Cavicchi et al., 1971; Chinzei, 1982; Broglio Loriga and Posenato, 1996). *Lithiotis* and
112 *Cochlearites* have dorso-ventrally elongated shells, with a thick attached valve and a thinner free
113 valve. In *Lithiotis*, the free valve is very thin and thus rarely preserved. *Cochlearites* is
114 characterized by an umbonal area with a median large furrow on the thicker valve and a median
115 ridge on the thinner valve. *Lithiotis* is distinguished from *Cochlearites* in having a body cavity with
116 a sub-central ridge in the thicker valve and a furrowed median plate (a possible multivincular
117 ligament area) on the umbonal area. *Lithioperna* is characterized by large, flattened to concavo-
118 convex shells with roundish to subrectangular outline. In radial longitudinal sections, the articulated
119 shells of *Lithioperna* have a flattened shape with the a couplet of lens-shaped articulated pair valves
120 which seemingly reflect one another.

121 *Cochlearites* and *Lithiotis* were semi-infaunal suspension-feeders, which developed a “mud-
122 sticker” strategy for stabilization in soft substrates in calm environments with relatively high
123 sedimentation rates (Chinzei, 1982; Seilacher, 1984). These taxa were cemented in the early life
124 stage to hard substrates. *Lithiotis* and *Cochlearites* shells are rarely found as bouquet-like
125 aggregates suggesting that their life position was basically up-right (Göhner, 1980; Chinzei, 1982;
126 Posenato et al., 2018). Their accumulations are characterized by a mud-supported core with a
127 loosely packed shells fabric with embedded congregation of forms (constratal *sensu* Skelton et al.,
128 1995) and few shells in vertical position. These build-ups, lacking a wave-resistant rigid framework,
129 have been defined as bivalve mounds (*sensu* Riding, 2002; Posenato and Masetti, 2012).

130 *Lithioperna* had an epifaunal to semi-infaunal mode of life. Two main morphotypes were
131 recognized in adult shells (Seilacher, 1984): an orthothetic, mud-sticker (morphotype A of Broglio
132 Loriga and Posenato, 1996), with a flat and thin shell contributing to crowded, book-like vertically
133 embriated colonies. and a pleurothetic morphotype, cup-shaped recliner (morphotype B of Broglio
134 Loriga and Posenato, 1996) with thick and roundish shells which lived in more sparse populations.
135 The morphotype B had either heavyweight shells for bottom stabilization in skeletal supported
136 substrates or corresponding lightweight strategies in mud-supported substrates (Broglio Loriga and
137 Posenato, 1996).

138

139 **3. Geological and stratigraphic setting**

140

141 The Calcarei Grigi Group represents a Hettangian–Pliensbachian carbonate shallow water
142 succession of the Trento Platform (Fig. 1), a palaeogeographic unit resulting from rifting associated
143 with the opening of central North Atlantic Ocean (e.g., Winterer and Bosellini, 1981; Castellarin et
144 al., 2005). In the study area, the Calcarei Grigi Group consists of the (in stratigraphic order):
145 Formazione di Monte Zugna, Calcare Oolitico di Loppio, Formazione di Rotzo, and the Oolite di
146 Massone (e.g., Castellarin et al., 2005).

147 The Formazione di Rotzo is characterized, in the lower part, by decimetre-thick grey peloidal
148 wackestone/packstone and marlstone alternations followed, in the upper part, by prevailing
149 packstone/grainstone calcarenites of packstone/grainstone with peloids or coated grains. It extends
150 from the Adige Valley to the Asiago area with the maximum thickness (ca. 250 m) in the Altopiano
151 di Tonezza–Folgaria area. The Formazione di Rotzo represents a tropical lagoon protected from the
152 open sea by oolitic shoals and from the emerged land by marshes (Bosellini and Broglio Loriga,
153 1971; Clari, 1975). Due to the scarcity of ammonoids, the biostratigraphy of the Formazione di
154 Rotzo has been essentially based on benthic foraminifera (e.g., Bosellini and Broglio Loriga, 1971;
155 Fugagnoli, 2004). The Formazione di Rotzo has been divided into three foraminiferal
156 biostratigraphic units (Fig. 2): *Lituosepta recoarensis* Zone, *Orbitopsella* Zone and *Lituosepta*
157 *compressa* Zone, ranging in age from the late Sinemurian to the late Pliensbachian (e.g., Fugagnoli,
158 2004).

159 The stratigraphic and geographical distribution of lithiotids in the Formazione di Rotzo were
160 controlled by various environmental factors (e.g., salinity, oxygen, hydrodynamic and trophic
161 regimes; Posenato and Masetti, 2012). *Lithiotis* is common in the middle part of the formation
162 (*Orbitopsella* Zone), where the foraminiferal assemblage suggests prevailing mesotrophic
163 conditions (Fugagnoli, 2004). The acme of lithiotid occurrence, mainly represented by *Cochlearites*,
164 occurs in the upper part of the formation, where prevailing oligotrophic conditions occurred
165 (Fugagnoli, 2004; Posenato and Masetti, 2012; Franceschi et al., 2014). *Lithioperna*, widespread
166 throughout the Formazione di Rotzo, is considered to be the most eurytopic lithiotid adapted to
167 more stressed (e.g., low oxygenation) environments in comparison to *Lithiotis* and *Cochlearites*
168 (Posenato et al., 2000; Fraser et al., 2004; Posenato and Masetti, 2012). Several studies dealt with
169 the facies characterising of this lithostratigraphic unit (Fugagnoli, 1999, 2004; Boomer et al., 2001;
170 Monaco and Giannetti, 2002; Bassi et al., 2008, 2015; Posenato et al., 2013a, 2013b).

171 The studied lithiotid shell deposits are defined as accumulations to indicate bivalve deposits
172 with no structural and dynamic implications (e.g., Riding 2002). Eighteen lithiotid accumulations
173 cropping out in the Verona, Vicenza and Trento areas (northeast Italy) were studied (Fig. 1, Table
174 1): one accumulation in the Vaio dell'Anguilla (Monti Lessini, Verona), seven accumulations in the

175 Altopiano di Tonezza (Vicenza; six in the Monte Toraro succession, one near Monte di
176 Campoluzzo), four accumulations in the Altopiano di Asiago (Vicenza), an isolated outcrop near
177 Passo Vezzena (Trento) with four lithiotid accumulations and a huge accumulation near Contrada
178 Dazio (Folgaria, Trento).

179

180 **4. Methods**

181

182 The studied lithiotid shell deposits are defined as accumulations to indicate bivalve deposits
183 with no structural and dynamic implications (e.g., Riding 2002). Eighteen lithiotid accumulations
184 cropping out in the Verona, Vicenza and Trento areas (northeast Italy) were studied (Fig. 1, Table
185 1): one accumulation in the Vaio dell'Anguilla (Monti Lessini, Verona), seven accumulations in the
186 Altopiano di Tonezza (Vicenza; six in the Monte Toraro succession, one near Monte di
187 Campoluzzo), four accumulations in the Altopiano di Asiago (Vicenza), an isolated outcrop near
188 Passo Vezzena (Trento) with four lithiotid accumulations and a huge accumulation near Contrada
189 Dazio (Folgaria, Trento).

190 The studied accumulations, characterised by the three most aberrant taxa (*Lithiotis*,
191 *Cochlearites*, *Lithioperna*), occur in six different successions, within the Formazione di Rotzo and
192 range from the *Orbitopsella* Zone to the *Lituosepta compressa* Zone (Fugagnoli 2004; Fig. 2, Table
193 1). These accumulations were selected for their distinctive characteristics which represent the suite
194 of the larger bivalve accumulations. The Monte Toraro, Monte di Campoluzzo and Vaio
195 dell'Anguilla outcrops, located in the middle-upper Formazione di Rotzo, show the accumulation
196 shapes in which all lithiotid morphotypes occur (Figs. 3–5). The Formazione di Rotzo accumulation
197 case shows horizontally oriented shell accumulations, with no defined general shape. The largest
198 accumulation occurs in Contrada Dazio outcrop (Göhner 1980), where the lithiotid shells are
199 chaotically arranged, while The Passo Vezzena outcrop has never been examined in detail.

200 The examined bivalve accumulations were described in terms of stratigraphic location,
201 dominant lithiotid taxa, shell fabrics and taphonomic attributes. These attributes are (1) percentage
202 of shell cover (% of area covered by shells), (2) shell density (number of individuals/400 cm²
203 occurring in perpendicular sections to the bedding or on the bedding surface), (3) percentage of
204 articulated and (4) complete shells, and (5) occurrence relative proportion of
205 autochthonous/parautochthonous or allochthonous individuals. Some representative randomly-
206 sectioned shell specimens allowed for the taxonomic identification of the dominating bivalve taxa
207 (see Posenato et al. 2018). Large rock samples were also sectioned and polished in order to identify
208 enclosed specimens. The sedimentary fabric and taphonomic attributes of the lithiotid
209 accumulations were quantitatively assessed using field macro-photographs of exposed natural rock

210 surfaces oriented either parallel or perpendicular to the bedding and analysed by using the graphic
211 software package AutoCAD 2004.

212 Each outcrop was mapped by quadrants (Fig. 3) in order to analyse the sedimentary and
213 taphonomic attributes of the lithiotids within the accumulations. Whenever possible, representative
214 quadrants were taken from the core and flanks of accumulations. In outcrops with undetermined
215 accumulation architecture (i.e., Rotzo, Contrada Dazio), randomly distributed quadrants were taken
216 from different parts of the accumulation. Depending on maximum shell size, quadrants ranging in
217 size from 7.5x7.5 cm to 40x40 cm were analysed. In all, a total of 150 quadrants were analysed
218 (Table 1) with the average values reported in Figs. 6–8.

219

220 **5. Results**

221

222 *5.1. Monte Toraro accumulation A (TorA1–A2, Figs 4A–B, 5, 6A)*

223

224 *Lithiotis* characterises two superimposed bivalve accumulations consisting of peloidal-
225 bioclastic rudstones/floatstones with a wackestone/packstone matrix containing rare undetermined
226 litiolid larger foraminifera: TorA1 and TorA2. TorA1 accumulation is ca. 1 m high and ca. 10 m
227 wide (Fig. 6A). The thick *Lithiotis* shells ranging from 5 mm to 25–30 mm in thickness and up to
228 30 cm high, are easily recognizable by the transversal sections of the body cavity of the attached
229 valve. The free valve, thinner than the attached one, cannot be identified at the outcrop scale.
230 Vertical and strongly inclined individuals are mostly preserved as moulds and casts due to aragonite
231 dissolution (Posenato and Masetti 2012, fig. 7g, k, l). In the TorA1 accumulation core the shell
232 density is relatively low (7–15 ind./400 cm²), but higher in the accumulation flanks (19–27 ind./400
233 cm²; Fig. 4B). The percentage of shell cover increases toward the accumulation flanks, where rare
234 sponges, brachiopods, *Pseudopachymytilus*, *Opisoma* and solitary corals occur. The core is
235 characterized by abundant autochthonous *Lithiotis* and brachiopod shells. The lithiotid shells have
236 an inclination ranging from 25°–30° to 80°; some bouquet-aggregates are also present (Fig. 4A). In
237 the periphery of the flanks, the shells are sub-horizontal (at most inclined ca. 15°; Fig. 4B).

238 The smaller lens-shaped A2 accumulation (Figs. 5, 6A), ca. 4 m wide and 30 cm high, is
239 dominated by wide, short and articulated *Lithiotis* shells (ca. 10 cm high and ca. 8 cm wide; Fig. 5).
240 Subordinate components are represented by brachiopods, larger foraminifera, oncoids and peloids.
241 The *Lithiotis* shells are sparse and sub-vertical in orientation.

242

243 *5.2. Monte Toraro accumulation B (TorB, Fig. 6B)*

244

245 This accumulation, 30 cm high in the core and ca. 10 m wide, consist of small *Cochlearites*
246 shells (up to 10–15 cm in height) in a bioclastic wackestone sediment matrix (Fig. 6B). Locally few
247 gastropods, rare solitary corals and rare thin-shelled bivalves are present (Posenato and Masetti
248 2005, 2012, fig. 7o).

249 In the core, the *Cochlearites* shells show complete dissolution while those occurring in the
250 accumulation flanks are re-crystallised. The shells occur in sub-vertical position, with rare bouquet-
251 like aggregates. In the core, because the bad preservation of the shells, articulated individuals were
252 not recognised. The shell density ranges from 60 ind./400 cm² in the core to 100 ind./400 cm²
253 towards the flanks (Fig. 6B). The flanks are characterized by a lower percentage of whole shells
254 (24.2%) than in the accumulation core (44.4%).

255

256 5.3. Monte Toraro accumulation C (TorC, Fig. 6D)

257

258 This accumulation, lying on a storm deposit with thin-shelled bivalves and gastropods, is ca.
259 15 m wide and ca. 1.5 m thick. *Cochlearites*, up to 2 cm thick and 10–15 cm up to 30 cm in height,
260 dominates. In the wackestone matrix, the shells are completely recrystallized. At the outcrop scale
261 (about 5 m wide), this accumulation shows a tabular shape (Fig. 6D). The accumulation flanks are
262 not clearly detectable. The shell fabric varies within the accumulation and most of the individuals
263 show an apparently chaotic arrangement with shell inclination ranging from few degrees to more
264 than 50°. Shell density and shell cover are highly variable (17–46 ind./400 cm² and 17–30%,
265 respectively). Two bouquet-like aggregates were also identified. The morphoplasticity (i.e.,
266 ontogenetic shell adaptation to the substrate) of the shells is shown by autochthonous individuals,
267 with the lowermost part of the shell sub-parallel and the uppermost part sub-vertical to bedding.

268

269 5.4. Monte Toraro accumulation D (TorD, Figs 4E, 6C)

270

271 This accumulation is tabular in shape, occurring at the bottom of a lens-shaped *Cochlearites*
272 accumulation, consists of decimetre-thick undulated packstone beds separated by erosional surfaces
273 (Fig. 4E, 6C). Dominating *Lithioperma* occurs as small (up to 8 cm in size) fragmented and
274 disarticulated shells. These are frequently iso-oriented and sub-parallel (10°) to the bedding. Low
275 percentage of articulated (ca. 5%) and whole shells (2–17%) and high shell density (220–252
276 ind./400 cm²) characterize this accumulation. Rare oncoids, brachiopods and gastropods are also
277 present.

278

279 5.5. Monte Toraro accumulation E (TorE, Fig. 7A)

280

281 This lens-shaped shell accumulation is dominated by recrystallized *Cochlearites* shells. In
282 the central accumulation area these shells, up to 20 cm long, are apparently sub-horizontally
283 arranged because they are transversally sectioned. Along the flanks the shells are longitudinally
284 sectioned and show an inclination of more than 30° (Fig. 7A). Locally rare individuals of
285 *Lithioperna* occur. Small brachiopods, rare solitary corals and gastropods are also present. The shell
286 density increases toward the lateral areas (from 10 to 27 ind./400 cm²). The same trend is followed
287 by the percentage of shell cover (from ca. 10% to 36%; Fig. 7A).

288

289 5.6. Monte di Campoluzzo accumulation (Cm, Figs 4F, 7B)

290

291 This accumulation is made up by *Lithioperna* morphotype A, with flattened, sub-equivalve
292 and slightly undulated shells (Figs. 4F, 7B). These are preserved as coarse calcitic prisms. Rare
293 individuals of *Cochlearites* occur as very small, disarticulated and sub-horizontal shells. Rare
294 brachiopods, gastropods and thin-shelled bivalves are also present.

295 Shell inclination varies from mainly sub-horizontal, to ca. 30° in the central part of the
296 outcrop, up to 70° in its outermost part. The shell density ranges from ca. 39–66 ind./400 cm² in the
297 central part to >100 ind./400 cm² in its periphery. The central area is characterized by high
298 percentage of articulated individuals (ca. 82%; even if recorded in some restricted areas) and the
299 occurrence of some whole shells (8–25%). The abundant lithiotid fragments contribute, therefore, to
300 the high shell density.

301

302 5.7. Vaio dell'Anguilla accumulation (Va, Fig. 7C–D)

303

304 The two lithiotid accumulations located ca. 6 m and ca. 20 m above the base of the
305 formation (Posenato and Masetti, 2012, fig. 5). Both accumulations are dominated by *Lithioperna*
306 morphotype A with densely packed vertically-subvertically arranged shells. In the first
307 accumulation, because the lower part is poorly preserved, the shell density and percentages of
308 whole and articulated shells were tentatively calculated (Fig. 7C). In the middle to upper part of the
309 accumulation, closely-packed, large shells are sub-horizontally arranged with a high percentage of
310 articulated and whole individuals. The second accumulation is similar to the the first with high shell
311 densities (ca. >30 ind./400 cm²) and a high percentage of articulated and whole shells (ca. >55%
312 and >30% respectively; Fig. 7D). Rare shell fragments locally occur.

313

314 5.8. Rotzo accumulations (Ro)

315

316 In this succession, the lithiotid bearing outcrops are some tens of meters in width. The
317 studied accumulations correspond to the Ro22, Ro27 and Ro34 units of Bosellini and Broglio
318 Loriga (1971). These beds are characterized by *Lithiotis*, *Cochlearites* and individuals tentatively
319 assigned to *Lithioperna* (Table 2).

320 The lower part of unit Ro22 contains *Lithiotis*, with a maximum shell size of ca. 20 cm long
321 and up to 1 cm thick. Shell density (13 ind./400 cm²) and shell cover (28.56%) are relatively low
322 (Table 2). Shells are randomly arranged ranging from sub-horizontal individuals to inclined shells.
323 Only larger individuals are articulated.

324 A tripartite subdivision is present in unit Ro27, 3 m in total thickness (Bosellini and Broglio
325 Loriga, 1971). In the micritic lower subunit (1.5 m thick), *Cochlearites* dominates with subordinate
326 *Lithioperna*. Rare gastropods are also present. The lithiotid shells are small in size (ca. 5–6 cm in
327 height high and only a few millimetres thick). Shell inclination ranges from 30°–40° in the lower
328 part to subhorizontal in the upper part. Shell density and shell size increase both laterally and
329 vertically. The average shell density is high (112 ind./400 cm²). The middle subunit (in total 1.45 m
330 thick), consist of several lithiotid bearing layers intercalated with bioclastic micritic beds, about 20–
331 40 cm thick with rare lithiotid shells. Each lithiotid layer is marked by undulated surfaces
332 interpreted as synsedimentary erosional events. The uppermost subunit (ca. 40 cm thick) contains
333 highly concentrated, iso-oriented ?*Lithioperna* shells, with shell inclinations changing laterally from
334 25° up to horizontal. Taphonomic attributes are difficult to assess in the middle and upper subunit
335 due to poor preservation.

336 The Ro34 (ca. 10 m in thickness) was subdivided in four parts by Bosellini and Broglio
337 Loriga (1971; Table 2). The unit consists of thick lithiotid accumulations with a micritic matrix
338 (Bosellini and Broglio Loriga, 1971). The muddy intervals Ro34.1 and Ro34.2 (lower part) are
339 dominated by *Cochlearites* with rare *Lithioperna*. The shell density is high (30–52 ind./400 cm²;
340 Ro34-section in Table 2) and the shells arrangement is chaotic. Sub-horizontal individuals and rare
341 bouquet-like aggregates are also present. Some bouquet-like aggregates were identified. Ro34-
342 section and Ro34-surface show the same shell density (Table 2), while the shell covered is biased
343 by the poor shell surface preservation.

344

345 5.9. Contrada Dazio accumulation (Da)

346

347 In the Contrada Dazio, lithiotid accumulations occur crop out in an extensive outcrop, ca. 30
348 m wide and high (Göhner, 1980). The analysed sedimentary body is wedge-shaped and only the
349 lower 2 m were previously described (i.e., Interval A of Göhner, 1980). In this accumulation, the

350 lithiotid shells are recrystallized and the core and flanks are not clearly distinguishable. *Lithiotis*
351 dominates and is associated with subordinate *Cochlearites*. Both *Lithiotis* and *Cochlearites* are
352 randomly arranged, with some individuals in an up-right position. Random shell sections and poor
353 exposure conditions did not allow for the assessment of articulation. In the analysed quadrants, the
354 percentage of complete shells does not show significant changes, while shell density increases
355 towards the periphery (Da3–4; Table 2).

356

357 5.10. Passo Vezzena accumulations (Ve, Figs 4C–D,8)

358

359 The studied lithiotid outcrop is located along the road connecting Asiago (Vicenza) to
360 Lavarone (Trento; Fig. 1). The outcrop, about 20 m wide and 3 m high, is composed of four
361 superimposed accumulations with packstone matrix dominated by *Cochlearites* (Ve1–4; Fig. 8A).
362 In Ve1 *Cochlearites* shells are chaotically to sub-vertically arranged (Figs. 4C, 8B). Rare
363 gastropods are also present. The percentage of articulated and complete shells is relatively low (ca.
364 2.13% and 8.91% respectively). Ve2 is characterized by vertical or slightly inclined *Cochlearites*
365 shells. The estimation of the shell covered areas and the complete shells is highly influenced by the
366 bad preservation of the outcrop (Fig. 8C). The shells are densely packed with complete, articulated
367 individuals, up to 20 cm in height and up to ca. 1 cm in thickness. The *Cochlearites* dominated
368 accumulations Ve3 and Ve4 show sub-horizontally and sub-vertically arranged large shells (up to
369 35 cm in height) with high percentage of complete, articulated individuals (>40%). *Lithioperna* is
370 subordinated. These last two accumulations are characterized by high densities of shells (ca. 48%;
371 Figs. 4D, 8D–E).

372

373 6. Discussion

374

375 Autochthonous *Cochlearites* and *Lithioperna* can occur both in the accumulation core and
376 flanks while autochthonous *Lithiotis* only occurs in the accumulation cores (es. Figs. 4A, 6A, 9;
377 Table 3). Among the studied accumulations, TorA1–A2 represents the best example of an
378 accumulation core where dominating autochthonous *Lithiotis* occurs in sub-vertical position or in
379 bouquet-like aggregates (Figs 4A–B). The high percentage of complete *Lithiotis* shells (i.e., ca.
380 87%; Table 2) and their sub-vertical arrangement in the accumulation core of Contrada Dazio is
381 also an indication for the autochthonous position of these bivalves.

382

383 *Cochlearites* typically occurs upright within dense thickets and bouquets, whereby the
384 commissure planes are oriented in various directions (Debeljak and Buser, 1998; Brame et al.,
2019). Bouquet aggregates of *Cochlearites* were found in the cores of TorC, TorB and Ve1–2.

385 These aggregates along with sub-vertical individuals are interpreted to be in life position (Chinzei
386 1982; Seilacher 1984). Similar as that described for rudists (Skelton et al., 1995) this arrangement
387 suggests a relative sparse availability of suitable attachment substrates. The best examples of
388 autochthonous *Cochlearites* shells are present in the Ve1–2 accumulations where they are complete,
389 articulated and in a vertical or slightly inclined orientation (Fig. 4C–D). Sparse, small *Cochlearites*
390 bouquets were also identified along the Ro34 accumulation flanks.

391 Autochthonous *Lithioperna* morphotype A showing the classic, highly-packed, book-like
392 vertically embricated accumulations (e.g., Seilacher, 1984; Broglio Loriga and Posenato, 1996)
393 were encountered in the core of the Vaio dell’Anguilla accumulation. The highly-packed
394 aggregation together with the semi-infaunal life habits are highly conducive to burial and
395 preservation and show corresponding high numbers of complete and articulated shells (Fig. 7C–D).
396 This type of preservation is common in the Trento Platform (Posenato and Masetti, 2012) and
397 Apennine Carbonate Platform of southern Italy (Posenato et al., 2018). In some cases, imbricated
398 autochthonous shells acted as hard substrates for the larval settlement of *Cochlearites*
399 accumulations (Posenato and Masetti, 2012, fig. 7c).

400 Inclined lithiotid shells found along the accumulation flanks are interpreted as
401 parautochthonous shells which have been displaced from their life position. These shells are often
402 correspondingly disarticulated and re-orientated, though they can remain complete (Table 3; Fig. 9).
403 The misplacement of the life position is likely due to a decrease of sedimentation rate and an
404 increase in water energy before final burial (e.g. Chinzei, 1982; Seilacher, 1984; Posenato and
405 Masetti, 2012). Encrusted and bioeroded shells of the lithiotid fauna are very rare. This suggests
406 that (1) sedimentation rates were high enough to hamper encrusting epifauna and bioeroding
407 endofauna and (2) parautochthonous to allochthonous lithiotid shells, which could have been
408 exposed for longer, to show increased encrustation and bio-erosion. The only detailed study on the
409 occurrence of bioerosion in a member of the lithiotid fauna suggested seasonal or temporal
410 mesotrophic conditions within an overall oligotrophic regime as a factors for this rare occurrence in
411 Pliensbachian larger bivalves (Bassi et al., 2017).

412 In the Ve3–4 accumulation, parautochthonous *Cochlearites* and *Lithioperna* individuals are
413 distinguished by high percentages of articulated shells along with large sizes and sub-horizontal
414 positions (Figs. 8D–E). These occurrences are interpreted as the flanks of two accumulations whose
415 cores are likely located lateral to the studied outcrop. The sub-horizontally arranged *Cochlearites* of
416 TorE are also interpreted as parautochthonous (Fig. 4E). If the accumulation core is surrounded by
417 radially arranged parautochthonous shells, their transversal sections appear as sub-horizontal. The
418 original inclination of the shells is undetectable since it depends to the randomly oriented section of
419 the outcrop. The increase in parautochthonous specimens may, therefore, suggest a change in the

420 above mentioned environmental parameters, which influenced the shell stability on the muddy
421 substrate.

422 Abundant parautochthonous forms are present in the accumulation flanks of the Monte di
423 Campoluzzo accumulation (Fig. 7B). The shell density (> 39 ind./400 cm²) and the flat and
424 ventrally elongated shell morphology are characteristics of the *Lithioperna* morphotype A (Fig. 4F,
425 7B). This morphotype, which lived vertically in life position, was adapted to high sedimentation
426 rates and contributed to very dense aggregates showing the typical vertically embricated book-like
427 (book-like in Seilacher, 1984) or bouquet-like (e.g., Fraser et al., 2004) packing arrangement.
428 Although shell inclination varies in the studied outcrops, the high percentage of articulated
429 individuals lying sub-horizontally and the occurrence of fragmented and disarticulated shells (Table
430 3, Fig. 9) suggest that accumulation flanks could be subjected to a higher water turbulence and
431 lower sedimentation rate than the autochthonous *Lithioperna* accumulations from the Vaio
432 dell'Anguilla (Figs. 7C–D). A weaker substrate anchorage (byssate at the juvenile stage) with
433 respect to the other lithiotids which are cemented as juveniles together with a reduced sedimentation
434 rate could have allowed *Lithioperna* to grow sub-horizontally (e.g., Broglio Loriga and Posenato,
435 1996, fig. 4F) thus reducing the possibilities of preserving shells in an up-right position.

436

437 6.1. Taphonomic attributes of the lithiotid accumulations

438

439 The analysis of the studied lithiotid accumulations allowed taphonomic attributes of bivalves
440 within the cores and flanks of bivalve accumulations to be assessed. The lithiotid accumulations
441 would have been exposed to processes of erosion, reworking and winnowing before final burial
442 (e.g., Nauss and Smith, 1988; Posenato and Masetti, 2012). These parautochthonous/allochthonous
443 accumulations show a high degree of spatial and temporal mixing, and thus represent within-
444 habitat, time-averaged assemblages (Kidwell et al., 1986). Despite the fact that the taxonomic
445 ascription of randomly sectioned specimens can be problematic, some general trends in preservation
446 of these bivalves can be recognized. Furthermore, the Monte Toraro, Monte di Campoluzzo, Passo
447 Vezzena and Vaio dell'Anguilla accumulations show nearly entire accumulation shapes (with both
448 core and flanks) and can thus be used as comparative models for the other outcrops such Rotzo and
449 Contrada Dazio which are not as well exposed. Distinctive sedimentary fabrics as well as
450 taphonomic features of the studied *Lithiotis*, *Cochlearites* and *Lithioperna* within the accumulation
451 core and flanks (Table 3; Fig. 9) can thus be compared.

452 The lithiotid accumulations with a tabular shape (Fig. 6C–D) yield both reworked
453 allochthonous shells (e.g., *Lithioperna*, TorD; Figs. 4E, 6C, 9) as well as
454 parautochthonous/autochthonous shells (e.g., *Cochlearites*, TorC; Fig. 6D). Allochthonous shell

455 accumulations are characterised by low shell cover (< ca. 18%), high shell density (>200 ind./cm²)
456 and very low percentages of articulated (< 6%) and complete bivalves (<17%) suggesting physical
457 reworking. This is the case for *Lithioperna* accumulation which represented the hard substrate for
458 the settlement of cemented or byssally attached bivalves. The tabular *Cochlearites* accumulation
459 (Fig. 6D) is comparable to those from the Apennine Carbonate Platform (Posenato et al., 2018).

460 Although adult specimens can also occur in the flanks, most lithiotid individuals in the core
461 represent the largest-sized adults. In the *Lithiotis* accumulations, the core is mud-supported, with
462 loosely packed shells of dominating autochthonous individuals (complete shells >15%) associated
463 with subordinate parautochthonous ones (e.g., Da, TorA1; Figs. 4A, 9). The muddy flanks show
464 higher shell cover and density, with well-preserved dominating sub-horizontal individuals (e.g.,
465 Ro22, TorA1; Fig. 4B). In the studied accumulation flanks, disarticulated *Lithiotis* shows a sub-
466 horizontal to inclined orientation (Table 3). These are interpreted as parautochthonous because their
467 interpreted life position was vertical to subvertical (e.g., Chinzei, 1982; Seilacher, 1984; Nauss and
468 Smith, 1988).

469 The *Cochlearites* accumulation core and flanks show a high variability of shell fabrics and
470 taphonomic attributes (e.g., Ve1–4; Table 3; Fig. 9). Only in Passo Vezzena outcrop (Ve1–2; Figs.
471 4C, 8B–C), is the core of the *Cochlearites* accumulation well preserved, with individuals in life
472 position (vertical/sub-vertical) with high shell densities. The flanks are characterized by inclined or
473 sub-horizontal shells whose taphonomic attributes vary according to the distance from the core area
474 (Ve3–4; Figs. 4D, 8D–E). As already noted in other localities (Posenato and Masetti, 2012), the
475 flanks constitute the most conspicuous part of the accumulation. The peripheral area shows higher
476 shell cover (>20%; TorE) and shell density (ca. > 17 ind./400 cm²; TorE; Fig. 7A) than the core
477 area. In the *Cochlearites* tabular bodies (e.g., TorC; Fig. 6D), the shell arrangement and taphonomic
478 attributes vary without a specific trend. In these bodies, sparse bouquet-like aggregates are present.
479 With regard to the Rotzo accumulations, the Ro27 (dominated by *Cochlearites*) and the Ro34
480 (dominated by *Cochlearites*) are interpreted as the accumulation flanks because their taphonomic
481 attributes (Table 2). *Cochlearites* records have been reported for southern Italy, Slovenia, Maorocco
482 and western USA (Debeljak and Buser, 1998; Fraser et al., 2004; Posenato et al., 2018; Brame et al.,
483 2019).

484 The single studied example of *Lithioperna* morphotype A accumulation core in the Vaio
485 dell'Anguilla accumulation, is characterized by highly dense packed shells with sub-
486 vertical/vertical arrangement. The accumulation core shows a high shell cover (ca. >47%), a high
487 percentage of articulated (ca. >55%) and complete shells (ca. >30%; Fig. 9). In the Monte di
488 Campoluzzo, the *Lithioperna* accumulation flanks show high shell cover (> 15%) and density (h >
489 15 ind./400 cm²), along with abundant parautochthonous individuals (Figs. 4F, 9; Table 3). In both

490 core and flanks, articulated shells occur in variable amounts (up to ca. 90%; Fig. 9). *Lithioperna*
491 accumulations described in the literature show generally a tabular shape (Posenato and Masetti
492 2012; Posenato et al. 2018), which can be related to the *Lithioperna* life habit (e.g., weak bottom
493 anchorage and shell instability), and environmental conditions (high hydrodynamic setting and low
494 sedimentary rate; Debeljak and Buser, 1998; Posenato and Masetti, 2012).

495

496 7. Conclusions

497

498 In the Pliensbachian shallow-water carbonate successions of the Southern Alps, northern Italy,
499 different types of lithiotid accumulations are present. Although the accumulations are often
500 characterized by wide lateral extension, only a limited number of outcrops allow for the recognition
501 of architectural features such as core and flanks. A quantitative taphonomic analysis was performed
502 in order to characterize these lithiotid accumulations and to explore the possibility of using
503 sedimentary fabrics and taphonomic features to distinguish accumulation core and flanks.

504 Based on taxonomic systematic composition, the accumulations can be dominated by a single
505 lithiotid species or be composed of the three species (i.e., *Lithiotis problematica*, *Cochlearites*
506 *loppianus*, *Lithioperna scutata*). When *Lithiotis* is the dominant taxon, it is rarely associated with
507 subordinate *Cochlearites*. Dominant *Cochlearites* is associated with subordinate *Lithioperna*. When
508 *Lithioperna* dominates, it occurs only with flat and thin shells and is rarely associated with
509 subordinate *Cochlearites*.

510 In the studied outcrops, autochthonous individuals in a vertical position or in a bouquet-like
511 aggregates are recognizable in the accumulation core, while the flanks are characterized by high
512 percentage of flat lying, toppled parautochthonous shells.

513 Shell bed characteristics and taphonomic attributes in the core and flanks vary according to the
514 dominating lithiotid bivalves: 1) in the core, the shell cover is highest for *Lithioperna*, variable for
515 *Cochlearites* and low for *Lithiotis*, while in the flanks these attributes show an opposite trend; 2)
516 shell densities are high in the core for *Cochlearites* and *Lithioperna* and low for *Lithiotis*, while in
517 the flanks it is high for all the taxa with more variability in *Cochlearites*; 3) articulated and
518 complete shells vary conspicuously in both the core and the flanks; 4) *Cochlearites* shows the
519 higher variability of taphonomic features; 5) a relative high percentage of articulated individuals
520 (>35%) of *Lithioperna* in the accumulation flanks suggests that autochthonous individuals also
521 thrived in these areas.

522 Supplementary data to this article can be found online at <http://doi.org/.....>

523

524

525 **Acknowledgements**

526

527 This study has been supported by the FAR2016–2018 and FIR2018 from the University of Ferrara.
528 This paper is a scientific contribution of the MIUR-Dipartimenti di Eccellenza 2018–2022 Project.
529 The authors are grateful to Thierry Correge, Matrias Reolid and Peter Skelton for helpful and
530 constructive comments.

531

532 **References**

533

534 Accorsi Benini, C., Broglio Loriga, C., 1977. *Lithiotis* Gümbel, 1971 e *Cochlearites* Reis, 1903 I–
535 Revisione morfologica e tassonomica. Boll. Soc. Paleontol. Ital. 16, p15–60.

536 Accorsi Benini, C., 1979. *Lithioperna*, un nuovo genere fra i grandi Lamellibranchi della facies a
537 “*Lithiotis*”. Morfologia, tassonomia ed analisi morfofunzionale. Boll. Soc. Paleontol. Ital. 18,
538 221–257.

539 Accorsi Benini, C., 1985. The large Liassic bivalves: symbiosis or longevity. Palaeogeogr.
540 Palaeoclimatol. Palaeoecol. 52, 21–33.

541 Accorsi Benini, C., Broglio Loriga, C., 1982. Microstrutture, modalità di accrescimento e
542 periodicità nei lamellibranchi liassici (facies a “*Lithiotis*”). Geol. Rom. 21, 795–823.

543 Bambach, R.K., 2006. Phanerozoic biodiversity mass extinction. Ann. Rev. Earth Plan. Sci. 34,
544 127–155.

545 Bassi, D., Fugagnoli, A., Posenato, R., Scott, D.B., 2008. Testate amoebae from the Early Jurassic
546 of the western Tethys, North-East Italy. Palaeontology 51, 1335–1339.

547 Bassi, D., Posenato, R., Nebelsick, J.H., 2015. Paleoecological dynamics of shallow-water bivalve
548 carpets from a Lower Jurassic lagoonal setting, northeast Italy. Palaios 30, 758–770, doi:
549 10.2110/palo.2015.020.

550 Bassi, D., Posenato, R., Nebelsick, J.H., Owada, M., Domenicali, E., Iryu, Y., 2017. Bivalve
551 borings in Lower Jurassic *Lithiotis* fauna from northeastern Italy and its palaeoecological
552 interpretation. Hist. Biol. 29, 937–946.

553 Berti Cavicchi, A., Bosellini, A., Broglio Loriga, C., 1971. Calcari a *Lithiotis problematica* Gumbel
554 o calcari a “*Lithiotis*”. Mem. Geopaleontol. Univ. Ferrara 3, 41–53.

555 Böhm, G., 1891. Über *Lithiotis problematica* Gümbel. Z. Dtsch. Geol. Ges. 43, 531–532.

556 Boomer, I., Whatley, R.C., Bassi, D., Fugagnoli, A., Broglio Loriga, C., 2001. An Early Jurassic
557 oligohaline ostracod assemblage within the marine carbonate platform sequence of the
558 Venetian Prealps, NE Italy. Palaeogeogr. Palaeoclimatol. Palaeoecol. 166, 331–344.

559 Bosellini, A., 1972. Paleoecologia dei Calcari a “*Lithiotis*” (Giurassico Inferiore, Prealpi Venete).
560 Riv. Ital. Paleontol. 78 (3), 441–464.

- 561 Bosellini, A., Broglio Loriga, C., 1971. I “Calcari Grigi” di Rotzo (Giurassico inferiore, Altopiano
562 di Asiago) e loro inquadramento nella paleogeografia e nell’evoluzione tettonico-sedimentaria
563 delle Prealpi Venete. Ann. Univ. Ferrara N. Ser. 9 (5/1), 1–61.
- 564 Brame, H.M.R., Martindale, R.C., Ettinger, N.P., Debeljak, I., Vasseur, R., Lathuilière, B., Kabiri,
565 L., Bodin, S., 2019. Stratigraphic distribution and paleoecological significance of Early
566 Jurassic (Pliensbachian–Toarcian) lithiotid-coral reefal deposits from the Central High Atlas
567 of Morocco. Palaeogeogr. Palaeoclimatol. Palaeoecol. 514, 813–837.
- 568 Broglio Loriga, C., Neri, C., 1976. Aspetti paleobiologici e paleogeografici della facies a “*Lithiotis*”
569 (Giurese inf.). Riv. Ital. Paleontol. Stratigr. 82 (4), 651–706.
- 570 Broglio Loriga, C., Posenato, R., 1996. Adaptive strategies of Lower Jurassic and Eocene
571 multivincular bivalves. Boll. Soc. Paleontol. Ital. spec. vol. 3, 45–61.
- 572 Buser, S., Debeljak, I., 1994. Lower Jurassic beds with bivalves in south Slovenia. Geologija 37,
573 23–62.
- 574 Castellarin, A., Picotti, V., Cantelli, L., Claps, M., Trombetta, L., Selli, L., Carton, A., 2005. Note
575 Illustrative della Carta Geologica D’Italia, foglio 080 Riva del Garda. APAT, Serv. Geol.
576 Italia, Firenze, pp. 1–145.
- 577 Chinzei, K., 1982. Morphological and structural adaptations to soft substrates in the Early Jurassic
578 monomyarians *Lithiotis* and *Cochlearites*. Lethaia 15, 179–197.
- 579 Clari, P., 1975. Caratteristiche sedimentologiche e paleontologiche di alcune sezioni dei Calcari
580 Grigi del Veneto. Mem. Ist. Geol. Min. Univ. Padova 31, 1–63.
- 581 Coen, L.D., Grizzle, R.E., 2016. Bivalve molluscs. In: Kennish, M.J. (ed.), Encyclopedia of
582 Estuaries. Springer, Netherlands, pp. 89–109.
- 583 Coletta, S., 2012. I bivalvi aberranti e microbiofacies della Formazione di Rotzo (Giurassico
584 Inferiore) dell’area del Valico di Valbona (Altopiano di Tonezza, Vicenza). Unpubl. M.Sc.
585 thesis, Univ. Ferrara, Ferrara, 87 pp.
- 586 Damborenea S.E., Echevarría J., Ros-Franch, S., 2017. Biotic recovery after the end-Triassic
587 extinction event: evidence from marine bivalves of the Neuquén Basin, Argentina.
588 Palaeogeogr. Palaeoclimatol. Palaeoecol. 487, 93–104.
- 589 Debeljak, I., Buser, S., 1998. Lithiotid bivalves in Slovenia and their mode of life. Geologija 40,
590 11–64.
- 591 Dera, G., Neige, P., Dommergues, J.-L., Fara, E., Laffont, R., Pellenard, P., 2010. High-resolution
592 dynamics of Early Jurassic marine extinctions: the case of Pliensbachian–Toarcian
593 Ammonites (Cephalopoda). J. Geol. Soc., 167, 21–33, 10.1144/0016-76492009-068
- 594 Dubar, G., 1948. La faune domerienne du Lias marocain (domaine atlasique). Notes Mem. Serv.
595 Géol. Maroc (Rabat) 68, 250 pp.

- 596 Franceschi, M., Dal Corso, J., Posenato, R., Roghi, G., Masetti, D., Jenkyns, H.C., 2014. Early
597 Pliensbachian (Early Jurassic) C-isotope perturbation and the diffusion of the *Lithiotis* Fauna:
598 insights from the western Tethys. *Palaeogeogr. Palaeoclimatol. Palaeoecol.* 410, 255–263.
- 599 Fraser, N.M., Bottjer, D.J., Fischer, A.F., 2004. Dissecting “*Lithiotis*” Bivalves: implications for the
600 Early Jurassic Reef Eclipse. *Palaios* 19, 51–67.
- 601 Fugagnoli, A., 1999. *Cymbriaella lorigae*, a new foraminiferal genus (Textulariina) from the Early
602 Jurassic of the Venetian Prealps (Northeastern Italy). *Rev. Micropaléontol.* 42 (2), 99–110.
- 603 Fugagnoli, A., 2004. Trophic regimes of benthic foraminiferal assemblages in Lower Jurassic
604 shallow water carbonates from northeastern Italy (Calcarei Grigi, Trento Platform, Venetian
605 Prealps). *Palaeogeogr. Palaeoclimatol. Palaeoecol.* 205, 111–130.
- 606 Geyer, O.F., 1977. Die “Lithiotis-Kalke” im Bereich der unterjurassischen Tethys. *Neues Jahrb.*
607 *Geol. Paläontol. Abh.* 153 (3), 304–340.
- 608 Gili, E., Skelton, P. W., Bover-Arnal, T., Salas, R., Obrador, A., Fenerci-Masse, M., 2016.
609 Depositional biofacies model for post-OAE1a Aptian carbonate platforms of the western
610 Maestrat Basin (Iberian Chain, Spain). *Palaeogeogr. Palaeoclimatol. Palaeoecol.* 453, 101–
611 114.
- 612 Göhner, D., 1980. „Covel dell'Angiolono“- ein mittelliassisches *Lithiotis*-Schlammbioherm auf der
613 Hochebene von Lavarone (Provinz Trento, *Norditalien*). *Neues Jahrb. Geol. Paläontol. Abh.*
614 10, 600–619.
- 615 Gümbel, C.W., 1871. Die sogenannten Nulliporen, *Lithiotis problematica*. *Abh. Königl. Bayer*
616 *Akad. Wiss. Cl.* 2 (1), 38–52.
- 617 Gutiérrez, J.L., Jones, C.G., Byers, J.E., Arkema, K.K., Berkenbusch, K., Commito, J.A., Duarte,
618 C.M., Hacker, S.D., Lambrinos, J.G., Hendriks, I.E., Hogarth, P.J., Andpalomo, M.G.. 2011.
619 Physical ecosystem engineers and the functioning of estuaries and coasts. In: Wolanski, E.,
620 McLusky, D.S. (Eds.), *Treatise on estuarine and coastal science*. Academic Press, Waltham,
621 vol. 7, pp. 53–81.
- 622 Gutiérrez, J.L., Jones, C.G., Strayer, D.L., Iribarne, O.O., 2003. Mollusks as ecosystems engineers:
623 the role of shell production in aquatic habitats. *Oikos* 101, 79–90, doi: 10.1034/j.1600-
624 0706.2003.12322.x.
- 625 Hallam, A., Wignall, P.B., 1997. *Mass extinctions and their aftermath*. Oxford Univ. Press, Oxford,
626 320 pp.
- 627 Hautmann, M., Stiller, F., Cai, H., Sha, J., 2008. Extinction-recovery pattern of level-bottom faunas
628 across the Triassic-Jurassic boundary in Tibet: implications for potential killing mechanisms.
629 *Palaios* 23, 711–718.

- 630 Kidwell, S.M., Fürsich, F.T., Aigner, T., 1986. Conceptual framework for the analysis and
631 classification of fossil concentrations. *Palaios* 1, 228–238.
- 632 Lee, C.W., 1983. Bivalve mounds and reefs of the Central High Atlas, Morocco. *Palaeogeogr.*
633 *Palaeoclimatol. Palaeoecol.* 43, 153–168.
- 634 Leinfelder, R., Schmid, D.U., Nose, M., Werner, W., 2002., Jurassic reef patterns – the expression
635 of a changing globe. In: Kiessling, W., Flügel, E., Golonka, J. (Eds.), *Phanerozoic Reef*
636 *Patterns*. SEPM Spec. Publ. 72, 465–520.
- 637 Mander, L., Twitchett, R.J., Benton, M.J., 2008. Palaeoecology of the Late Triassic extinction event
638 in the SW UK. *J. Geol. Soc. Lond.* 165, 319–332.
- 639 Martindale, R.C., Foster, R.J., Velledits, F., 2019. The survival, recovery, and diversification of
640 Metazoan reef ecosystems following the End-Permian mass extinction event. *Palaeogeogr.*
641 *Palaeoclimatol. Palaeoecol.* 513, 100–115.
- 642 Masetti, D., Claps, M., Giacometti, A., Lodi, P., Pignatti, P., 1998. I Calcari Grigi della Piattaforma
643 di Trento (Lias inferiore e Medio, Prealpi Venete): *Atti Ticinesi di Scienze della Terra*, v. 40,
644 p. 139–183.
- 645 Monaco, P., Giannetti, A., 2002. Three-dimensional burrow systems and taphofacies in shallowing-
646 upward parasequences, lower Jurassic carbonate platform (Calcari Grigi, Southern Alps, Italy).
647 *Facies* 47, 47–57.
- 648 Nauss, A.L., Smith, P.L., 1988. *Lithiotis* (Bivalvia) bioherms in the Lower Jurassic of east-central
649 Oregon, U.S.A. *Palaeogeogr. Palaeoclimatol. Palaeoecol.* 65, 253–268.
- 650 Parras, A., Casadío, A., 2006. The oyster *Crassostrea? hatchery* (Ortmann, 1897), a physical
651 ecosystem engineer from the upper Oligocene–lower Miocene of Patagonia, Southern
652 Argentina. *Palaios* 21, 168–186.
- 653 Posenato, R., Masetti, D., 2005. Stop 3. The *?Cochlearites* micromound of monte Toraro. In
654 Masetti et al. (Eds.), *The Rotzo Formation (Lower Jurassic at the Val Bona Pass (Vicenza*
655 *Province). Field Excursion book, 5th Reg. Symp. Int. Fossil Algae Ass., St. Trent. Sci. Nat.*
656 *Acta Geol.* 80 suppl., 23–25.
- 657 Posenato, R., Masetti, D., 2012. Environmental control and dynamics of Lower Jurassic bivalve
658 build-ups in the Trento Platform (Southern Alps, Italy). *Palaeogeogr. Palaeoclimatol.*
659 *Palaeoecol.* 361–362, 1–13.
- 660 Posenato, R., Masetti, D., Broglio Loriga, C., 2000. I banchi a bivalvi del Giurassico Inferiore
661 (Piattaforma di Trento): dinamica deposizionale, modalità di insediamento e sviluppo. In:
662 Cerchi, A., Corradini, C. (Eds.), *Crisi biologiche, radiazioni adattative e dinamica delle*
663 *piattaforme carbonatiche*. *Acc. Naz. Sci. Lett. Arti Modena* 21, 211–214.

- 664 Posenato, R., Bassi, D., Avanzini, M., 2013a. Bivalve pavements from shallow-water black-shales
665 in the Early Jurassic of northern Italy: a record of salinity- and oxygen-depleted
666 environmental dynamics. *Palaeogeogr. Palaeoclimatol. Palaeoecol.* 369, 262–271.
- 667 Posenato, R., Bassi, D. and Nebelsick, J.H., 2013b, *Opisoma excavatum* Boehm, a Lower Jurassic
668 photosymbiotic alatoform-chambered bivalve: *Lethaia*, v. 46, p. 424–437.
- 669 Posenato, R., Bassi, D., Nebelsick, J., 2014. Field Trip Guide – Tonezza del Cimone (VI)
670 13/09/2014. 7th Int. Meeting on Taphonomy and Fossilization, Taphos 2014, 10th–
671 13th/09/2014, Ferrara, Italy, 28 pp.
- 672 Posenato, R., Bassi, D., Trecalli, A., Parente, M., 2018. Taphonomy and evolution of Lower
673 Jurassic lithiotid bivalve accumulations in the Apennine Carbonate Platform (southern Italy).
674 *Palaeogeogr. Palaeoclimatol. Palaeoecol.* 489, 261–271.
- 675 Reis, O., 1903. Über Lithiotiden. *Abh. K.-K. Geol. Reich.* 17 (6), 1–44.
- 676 Riding, R., 2002, Structure and composition of organic reefs and carbonate mud mounds: concepts
677 and categories. *Earth-Sci. Rev.* 58, 163–231.
- 678 Ros, S., Echevarría, J. 2012. Ecological signature of the end-Triassic biotic crisis: what do bivalves
679 have to say? *Hist. Biol.* 24, 489–503.
- 680 Savazzi, E., 1996. Preserved ligament in the Jurassic bivalve *Lithiotis*: adaptive and evolutionary
681 significance. *Palaeogeogr. Palaeoclimatol. Palaeoecol.* 120, 281–289.
- 682 Seilacher, A., 1984. Constructional morphology of bivalves evolutionary pathways in primary
683 versus secondary soft dwellers. *Palaeontology* 27, 207–237.
- 684 Skelton, P.W., Gili, E., Vicens, E., Obrador, A., 1995. The growth fabric of gregarious rudist
685 elevators (hippuritids) in a Santonian carbonate platform in the southern Central Pyrenees.
686 *Palaeogeogr. Palaeoclimatol. Palaeoecol.* 119, 107–126.
- 687 Tausch, L., 1890. Zur Kenntnis der Fauna der “Grauen Kalke”. *Abh. K.-K. Geol. Reich.* 15 (2), 1–
688 40.
- 689 Trecalli, A., Spangenberg, J., Adatte, K., Föllmi, K.B., Parente, M., 2012. Carbonate platform
690 evidence of ocean acidification at the onset of the early Toarcian oceanic anoxic event. *Earth
691 Planet. Sci. Lett.* 357–358, 214–225.
- 692 Vilardell, O., Gili, E., 2003. Quantitative study of a hippuritid rudist lithosome in a Santonian
693 carbonate platform in the southern Central Pyrenees. *Palaeogeogr. Palaeoclimatol. Palaeoecol.*
694 200, 31–41.
- 695 Waldbusser, G.G., Steenson, R.A., Green, M.A., 2011. Oyster shell dissolution rates in estuarine
696 waters: effects on pH and shell legacy. *J. Shellfish Res.* 30, 659–669.
- 697 Wignall, P.B., Bond, D.P.G., 2008. The end-Triassic and Early Toarcian mass extinction records in
698 the British Isles. *Proc. Geol. Assoc.* 119, 73–84.

699 Winterer, H., Bosellini, A., 1981. Subsidence and sedimentation on Jurassic passive continental
 700 margin, southern Alps, Italy. Am. Assoc. Pet. Geol. Bull. 42, 394–419.

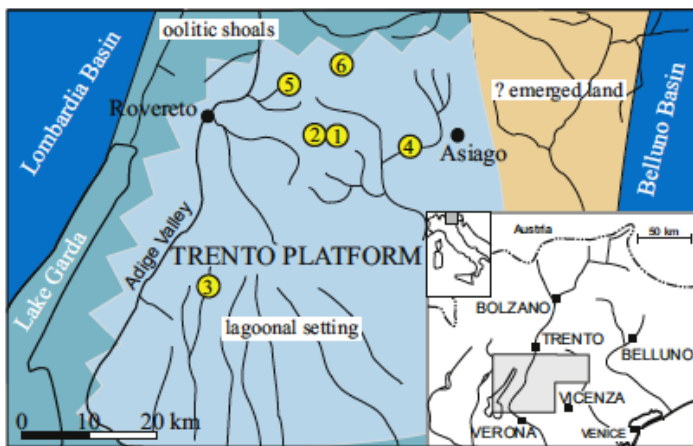
701

702 **Figure and table captions**

703

704 **Fig. 1.** Geographic locations of the studied lithiotid accumulations in the Trento Platform, northern
 705 Italy. 1, Monte Toraro; 2, Monte di Campoluzzo; 3, Vaio dell’Anguilla; 4, Rotzo; 5, Contrada
 706 Dazio; 6, Passo Vezzena. Palaeogeographic map from Posenato and Masetti (2012, modified).

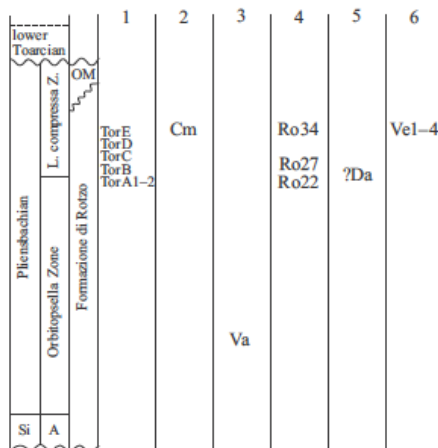
707



708

709

710 **Fig. 2.** Schematic stratigraphic setting of the Formazione di Rotzo with the biostratigraphic location
 711 of the studied accumulations. Numbers refer to the geographic areas of Fig. 1. Si, upper
 712 Sinemurian; A, *Lituosepta recoarensis* Zone; *L. compressa* Z., *Lituosepta compressa* Zone; OM,
 713 Oolite di Massone.

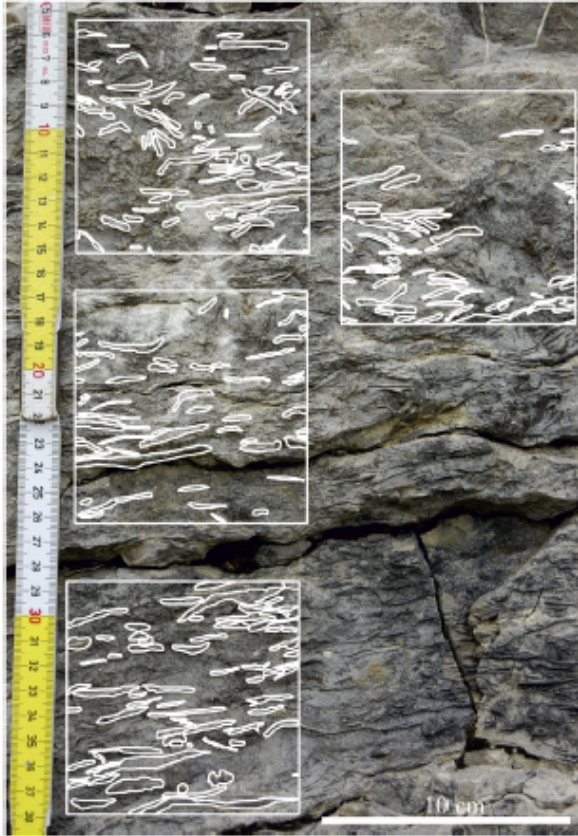


714

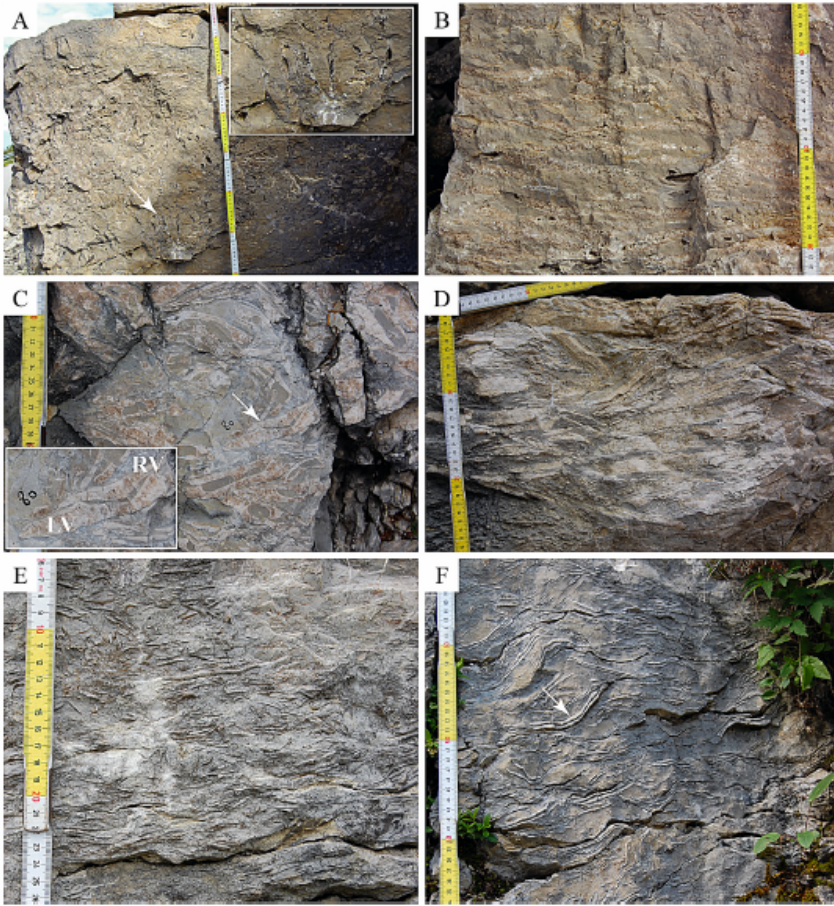
715

716 **Fig. 3.** Example of analysed quadrants in each of which with digitally analyzed photos in which the
 717 randomly sectioned lithiotid shells preserved within indurated limestone were traced (e.g.,

718 *Lithioperna*, TorD). In the digitally analyzed photos sedimentary fabrics and taphonomic attributes
719 such as percentage of shell cover, shell density, percentage of articulated and complete shells were
720 calculated.
721



722
723
724 **Fig. 4.** Examples of randomly-sectioned lithiotid specimens characterising the studied
725 accumulations. A–B, *Lithiotis problematica* (A, core with bouquet-like aggregate, circle inset white
726 rectangle; B, parautochthonous specimens in the accumulation flanks; TorA). C–D, *Cochlearites*
727 *loppianus* (C, core; D, flanks; Passo Vezzena), white arrows points to a cross-section of an
728 articulated shell which shows the free right valve (R.V.) with the internal median ridge (above) and
729 the thicker left valve (L.V.) characterized by a median wide furrow (below); e.g., Chinzei, 1982).
730 E–F, *Lithioperna scutata* (E, base of the accumulation, TorD; F, flank, Monte di Campoluzzo);
731 white arrow points to an articulated specimen with the characteristic shape resembling a couple of
732 lenses (e.g., Broglio Loriga and Posenato, 1996). White arrows point to random sections of
733 *Cochlearites* (C) and *Lithioperna* (F) showing the taxonomic diagnostic characters (see e.g.,
734 Chinzei, 1982).
735



736

737

738

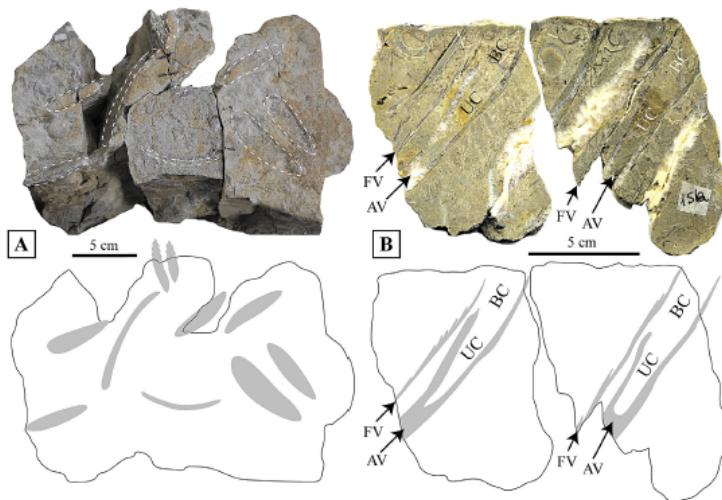
739

740

741

742

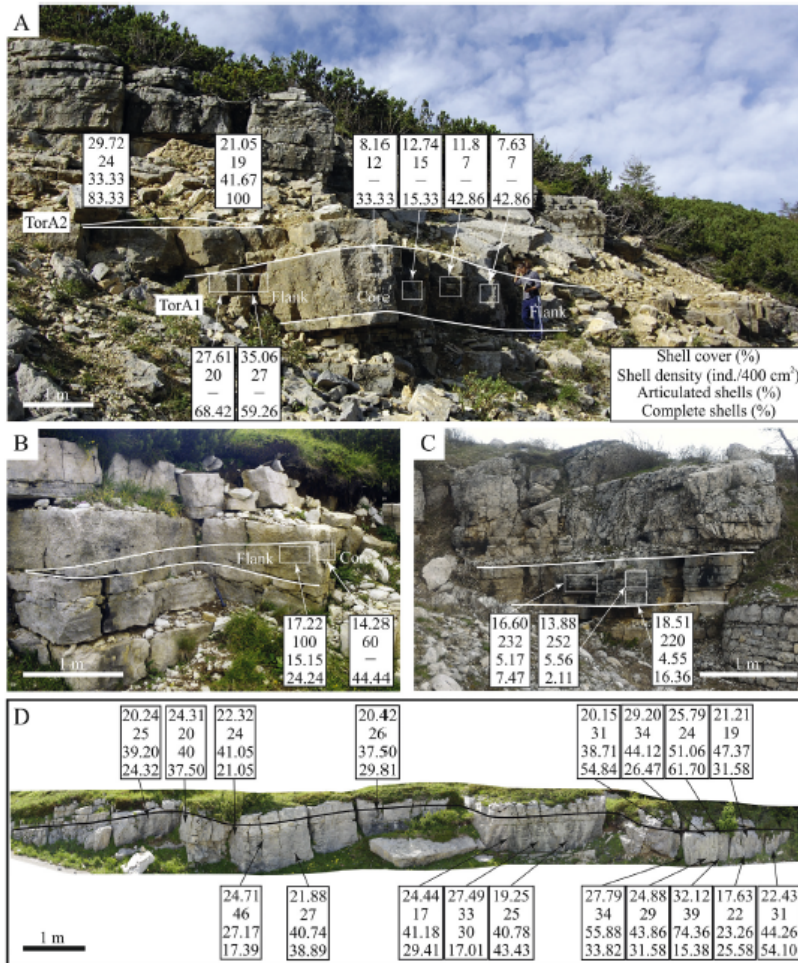
Fig. 5. Two rock samples representing mostly articulated and autochthonous *Lithiotis problematica* specimens from the accumulation TorA2. A) Upper bed surface with sub-transversal sections of the *Lithiotis* massive umbonal region. B) Polished surface of a perpendicular bedding section showing some articulated shells; two representative specimens are depicted with free (F.V.) and attached (A.V.) valves. B.C., body cavity; U.C., umbonal body cavity.



743

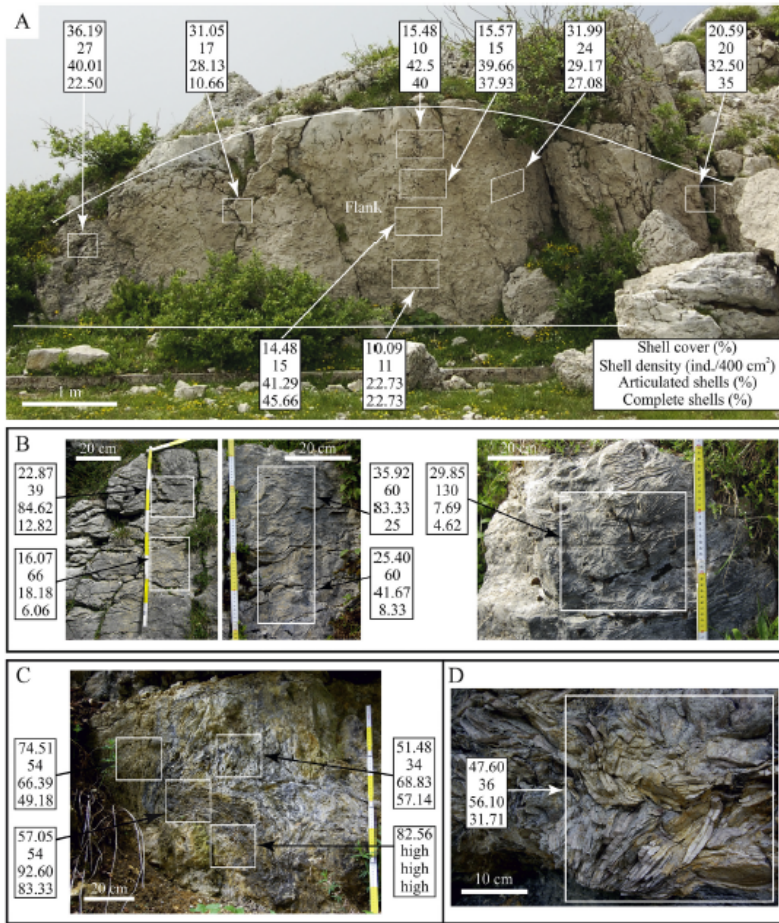
744

745 **Fig. 6.** Distribution of distinguished features in the Monte Toraro succession. The accumulations
 746 are marked by solid lines. A) TorA1–2. B) TorB. C) TorD. D) TorC. The TorD (C), characterized
 747 by *Lithioperna* shells, represents a tabular bioclastic, coarse-grained hard substrate for the overlying
 748 lithiotid accumulation.



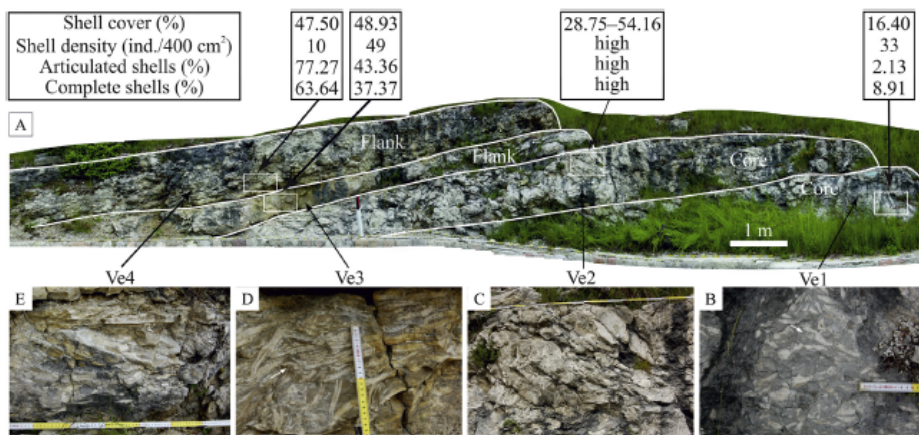
749
 750
 751 **Fig. 7.** Distribution of distinguished features in the studied lithiotid accumulations in the Monte
 752 Toraro (A, TorE), Monte di Campoluzzo (B) and Vaio dell'Anguilla (C–D) successions which are
 753 marked by solid lines. The studied TorE (A) represents a section of a *Cochlearites* accumulation
 754 passing only through the accumulation flank. The Monte di Campoluzzo (B) accumulation consist
 755 of parautochthonous *Lithioperna* individuals, while that of Vaio dell'Anguilla (C, D) consists of
 756 autochthonous *Lithioperna* individuals.

757



758
759
760
761
762
763
764

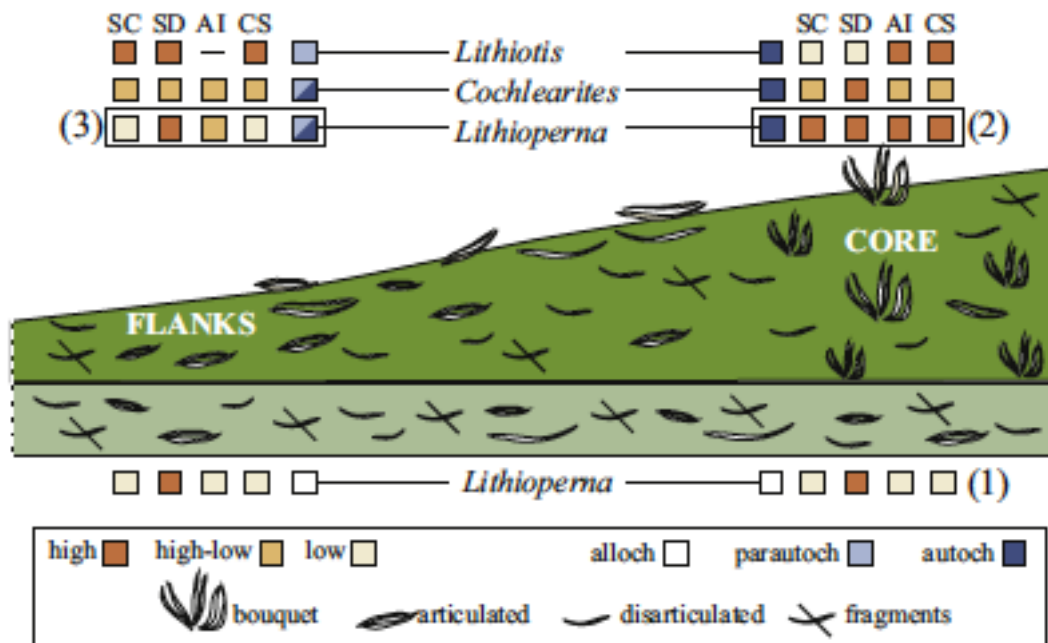
Fig. 8. Distribution of distinguished taphonomic features in the studied lithiotid accumulations in the Passo Vezzena (A–E) outcrop. The accumulations are marked by solid lines. White arrows point to random sections of *Cochlearites* showing diagnostic characters (see e.g., Chinzei 1982).



765
766
767
768

Fig. 9. Schematic model of the studied lithiotid accumulations showing the dominant distribution of the assessed fabric and taphonomic attributes of autochthonous (autoch), parautochthonous (parautoch), and allochthonous (alloch) shells.

769 (parautoch) and allochthonous (alloch) individuals. The tabular bioclastic hard-substrate (TorD),
 770 produced by physical reworking, is the representative study case made up of allochthonous
 771 *Lithioperna* shells (1; Fig. 6C). Autochthonous *Lithiotis* was found articulated in the level TorA2
 772 overlying the TorA1, whereas parautochthonous *Lithiotis* characterise the accumulation flank (Fig.
 773 6A). Autochthonous *Lithioperna* was recorded in the Vaio dell'Anguilla (2; Fig. 7C–D), while
 774 parautochthonous individuals of the Monte di Campoluzzo occur in the accumulation flank (3; Fig.
 775 7B). Not to scale. Lithiotid shells are simply depicted and do not reflect the complex shell
 776 morphology. SC, shell cover; SD, shell density; AI, articulated individuals; CS, complete shells.



777

778

779 **Table 1.**

780 Summary data of the studied lithiotid accumulations with the geographic and biostratigraphic
 781 locations, number of the total analysed quadrants and areal extension for each analysed quadrant.
 782 The distance of the studied accumulations from the base of the stratigraphic section refers to Coletta
 783 (2012; Monte Toraro, Monte di Campoluzzo), Posenato and Masetti (2012; Vaio dell'Anguilla) and
 784 Bosellini and Broglio Loriga (1971; Rotzo). Details of the shell accumulations in the text. Z., Zone.

Stratigraphic section	Accumulation	Distance from the base	Biozone	Total analysed quadrants	Area1 extension for each quadrant
Monte Toraro (45°52'08.9"N, 11°16'20.2"E)	TorA1	-120 m	<i>Orbitopsalla</i> Zone	15	400 cm ²
	TorA2	-120 m	<i>Orbitopsalla</i> Zone	4	100 cm ² (1), 56.25 cm ² (3)
	TorB	160 m	<i>L. compressa</i> Z.	2	100 cm ²
	TorC	172 m	<i>L. compressa</i> Z.	42	400 cm ²
	TorD	177 m	<i>L. compressa</i> Z.	9	100 cm ²
	TorE	180 m	<i>L. compressa</i> Z.	26	400 cm ²
Monte di Campoluzo (45°52'17.9"N, 11°15'34.4"E)	Cm	-1-2 m	<i>L. compressa</i> Z.	5	400 cm ²
Vaio dell'Anguilla (45°39'26.3"N 11°00'58.5"E)	Va	-15 m	<i>Orbitopsalla</i> Z.	5	900 cm ² (3), 400 cm ² (2)
Rotzo (45°51'06.7"N, 11°22'15.8"E)	Ro22	-60 m	<i>Orbitopsalla</i> Z.	3	400 cm ²
	Ro27	-68 m	<i>L. compressa</i> Z.	10	100 cm ²
	Ro34.1	-81 m	<i>L. compressa</i> Z.	1	400 cm ²
	Ro34.2	-82 m	<i>L. compressa</i> Z.	1	100 cm ²
	Ro34	Ro34 section Ro34 surface	-87 m -89 m	<i>L. compressa</i> Z. <i>L. compressa</i> Z.	1 10
Contrada Dazio (45°55'40.1"N, 11°15'31.8"E)	Da	Isolated outcrop	? <i>L. compressa</i> Z.	4	900 cm ²
Passo Vezzana (45°57'05.1"N, 11°21'36.3"E)	Ve1	Isolated outcrop	<i>L. compressa</i> Z.	3	400 cm ²
	Ve2	Isolated outcrop		6	1600 cm ² (4), 400 cm ² (1), 900 cm ² (1)
	Ve3	Isolated outcrop		2	400 cm ² (1), 225 cm ² (1)
	Ve4	Isolated outcrop		1	900 cm ²

785
786

787

788 **Table 2.**

789 Dominating lithiotid genera and average values of shell bed characteristics and taphonomic
790 attributes for the studied accumulations located in the Rotzo stratigraphic section (Ro) and Contrada
791 Dazio (Da). The percentages of articulated and complete shells in the Ro34-surface are tentatively
792 calculated (?) because the difficult in assessing articulated and/or whole individuals on bedding
793 surface. In Da1-4 the articulated individuals cannot be identified at the outcrop scale. *Cochl*,
794 *Cochlearites*; *Lithiop*, *Lithioperna*; -, no entry.

795

Shell beds	Dominating taxa	Shell cover (%)	Shell density (ind./400 cm ²)	Articulated shells (%)	Complete shells (%)
Ro22	<i>Lithiotis</i>	28.56	13	69.99	62.39
Ro27 (lower part)	<i>Cochlearites</i> (rare <i>Lithiop</i>)	52.95	112	16.24	21.44
Ro34.1	<i>Cochlearites</i> (rare <i>Lithiop</i>)	68.28	30	100	100
Ro34.2	<i>Cochlearites</i> (rare <i>Lithiop</i>)	61.41	52	83.33	36.67
Ro34-section	<i>Cochlearites</i> (rare <i>Lithiop</i>)	63.57	32	84.38	78.13
Ro34-surface	<i>Cochlearites</i> (rare <i>Lithiop</i>)	55.58	32	?	?10.56
Da1	<i>Lithiotis</i> (rare <i>Cochl</i>)	27.56	7	-	87.50
Da2	<i>Lithiotis</i> (rare <i>Cochl</i>)	22	11	-	87.50
Da3	<i>Lithiotis</i>	38.82	17	-	86.84
Da4	<i>Lithiotis</i>	31.95	17	-	86.84

796

797

798

799 **Table 3.**

800 Distinctive attributes for the core and flanks in the lithiotid accumulations. Autochthonous
801 individuals were preserved in life position, while parautochthonous were reworked to some degree,
802 but not transported out of the original life habit.

803 The obtained mean values differ among the dominating genera as follow (h, high): *Lithiotis*: shell
804 cover, h > 25%; shell density, h > 17 ind./400 cm²; articulated individuals, h > 35%; whole
805 individuals, h > 15%. *Cochlearites*: shell cover, h > 15%; shell density, h > 17 ind./400 cm²;

806 articulated individuals, $h > 35\%$; complete shells, $h > 35\%$. *Lithioperma* A (morphotype *sensu*
 807 Broglio Loriga and Posenato 1996): shell cover, $h > 40\%$; shell density, $h > 17$ ind./400 cm²;
 808 articulated individuals, $h > 35\%$; whole shells, $h > 25\%$.
 809

	Shell cover (%)	Shell density (ind./400 cm ²)	Articulated shells (%)	Complete shells (%)	Autochthonous individuals	Parautochthonous individuals
Core						
<i>Lithiotes</i>	Low	High-low	High	High	High	Low
<i>Cochlearites</i>	High-low	High	High-low	High-low	High	Low
<i>Lithioperma</i> A	High	High	High	High	High	Low
Flanks						
<i>Lithiotes</i>	High	High	-	High	-	High
<i>Cochlearites</i>	High-low	High-low	High-low	High-low	Low	High
<i>Lithioperma</i> A	Low	High	High-low	Low	Low	High

810
 811